



Improvements of the subgroup resonance calculation code SUGAR



Lei He, Hongchun Wu, Liangzhi Cao*, Yunzhao Li

School of Nuclear Science and Technology, Xi'an Jiaotong University, Xi'an, Shaanxi 710049, China

ARTICLE INFO

Article history:

Received 23 April 2013

Received in revised form 14 November 2013

Accepted 15 November 2013

Available online 20 December 2013

Keywords:

Subgroup method

Speed up

Iteration optimization

Grouping technique

ABSTRACT

Due to its accuracy and geometric flexibility, the subgroup method is becoming a more and more attractive resonance calculation approach dedicated to obtaining resonance group macroscopic cross sections from multi-group libraries. In order to increase the efficiency of our subgroup code SUGAR, this paper contributes to the development of the code from four aspects. Firstly, subgroup parameters were proved to be problem-independent and the number of subgroups can be chosen automatically. This motivated us to produce a new multi-group library. Secondly, what subgroup method really needs is the relative subgroup flux within each multi-group instead of the relative multi-group flux between different groups. Thus, it is unnecessary to iteratively calculate in the whole energy range if the connections between different energy ranges can be approximated by a simple method. Thirdly, for problems with complex isotope compositions, resonant nuclides could be grouped according to their resonance characteristics. By this grouping, computational effort could be significantly reduced since nominal resonant nuclides turn out to be these nuclide groups rather than the actual nuclides. Finally, considering that most of the computational effort is spent on solving the subgroup neutron transport equation, an in-house matrix MOC solver is employed to replace the AutoMOC solver. In this way, the higher speed of the matrix MOC solver can be fully utilized by our subgroup code. To verify these theories and to prove the improvements, a series of benchmark problems were solved. It is demonstrated by these numerical results that these techniques can accelerate the code SUGAR by a factor of 5–32 with respect to overall computations without losing accuracy and geometric flexibility. It was also found that the more complex the resonant nuclide composition is, the sharper the acceleration effect appears to be.

© 2013 Elsevier Ltd. All rights reserved.

1. Introduction

Resonance calculation is one of the most important steps for lattice calculation in nuclear reactor physics. Traditional resonance self-shielding calculation methods mainly include the equivalent theory employed by WIMSD4 (Trkov and Ravnik, 1993), CASMO-3 (Misu and Grummer, 1997) and DRAGON (Dahmani et al., 2008), the superfine group method (Ishiguro, 1973) employed by SRAC (Tsuchihashi, 1989). Both of them need to calculate the first flight collision probability. However, the first flight collision probability only can be obtained when the geometry is regular. So both two methods can only be used for simple geometry in traditional nuclear reactors.

As nuclear energy plays a more and more important role, several reactor concepts and nuclear devices are proposed and designed, which challenge the legacy resonance calculation methods. On one hand, differing from the traditional designs, most of them contain rigorous fuel types with complex geometries. Taking CANDU (Jeong and Suk, 2002) as an example, fuel assemblies are pressure tubes containing multiple fuel rods instead of rectan-

gular assemblies with only one single fuel rod in it. On the other hand, new fuel assemblies or other components usually contain complex isotope compositions including additional resonant nuclides such as Pu, Th, Gd, Er and I, which result in the resonance interference effect stronger than ever. For example, Er and I are usually considered as non-resonant nuclides in legacy PWRs while they have to be treated as resonant nuclides in reactors for minor actinides (MA) or long lived fission products (LLFP) transformation (Salvatores, 2005). In Fig. 1, a curve of I-129's microscopic cross section is shown following the continuous-energy. I-129 has large numbers of strong peaks in high energy region while it does not affect the computational accuracy in the ecumenical water cooled reactor and be considered as non-resonant nuclides. However, it is necessary to consider I-129 in the FP transformation calculation (He et al., 2010).

The increasing number of resonant nuclides not only requires the multi-group library to provide corresponding resonance data but also increases the computing efforts by making the multi-nuclide resonance iteration much more complicated. In this situation, the wavelet expansion method (Yang et al., 2010) can handle unstructured geometries and multi-nuclide resonance. However, its huge number of coefficient equations results in a relatively low efficiency (Le Tellier et al., 2009; Yang et al., 2010).

* Corresponding author. Tel./fax: +86 029 8266 8916.

E-mail address: caolz@mail.xjtu.edu.cn (L. Cao).

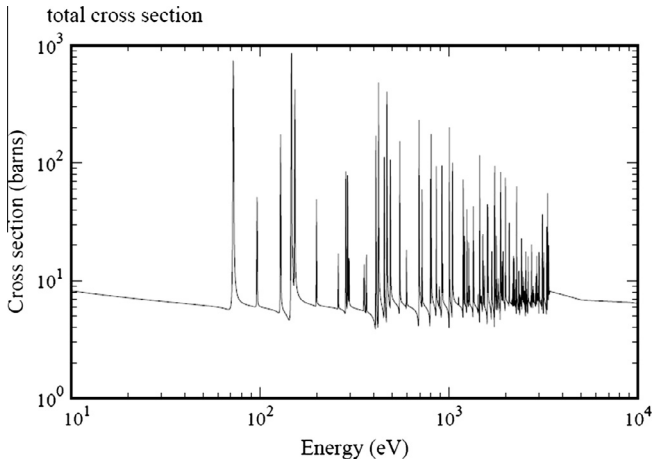


Fig. 1. Microscopic total cross section of I-129.

The subgroup method, advanced from 1990s by Takeda and Yokoyama (1997) and Hébert (2009) and currently implemented in DRAGON (Dahmani et al., 2008) and WIMS (Patrulescu et al., 1997) provides a novel perspective of getting the probability distribution of cross section for resonant nuclides. The subgroup method divides the cross section itself into several sections which are called the subgroups rather than to divide along with the energy variable. In addition to the ability of excellent accuracy, the neutron slowing down equation is transformed into a neutron-transport-equation-like equation without introducing any limitation to geometry treatments. Based on these two advantages, a subgroup code named SUGAR (Subgroup Universal Geometry Adaptable Resonance) has been developed in the NECP (Nuclear Engineering Computational Physics) laboratory by Liu (2010) and Cao et al. (2011). This code employs the classic subgroup theory and a MOC solver named AutoMOC (Chen et al., 2008) is involved to maintain the accuracy and geometry flexibility of subgroup method.

However, the efficiency of the code SUGAR appears to be insufficient mainly because of two reasons. The first is the frequent calls of the solver to solve the neutron-transport-equation-like slowing-down equation iteratively. The second is the appearance of more resonant nuclides such as Pu in the MOX fuel (Franceschini and Petrovic, 2008) and MA or LLFP in the transmutation targets. In order to increase the efficiency without losing the accuracy and geometric flexibility, this paper concludes four improvements on the SUGAR code. Section 2 introduces the theories of these improvements including: (1) Problem independent subgroup parameters are pre-calculated in a newly produced multi-group library with 361 energy groups. (2) Iteration simplification is made based on the facts that almost all the fission neutrons are generated into fast energy groups and that there is no up-scattering in resonance energy groups. (3) In the multi-nuclide resonance iterative calculation, the resonant nuclides are divided into several groups in order to solve the resonance interference more effectively. (4) The transport solver has been replaced by an advanced MOC solver. Section 3 lists and discusses the corresponding numerical results. Some conclusions are drawn in Section 4.

2. Theoretical model

2.1. Fundamentals of the subgroup method

Differing from the traditional self-shielding methods, the subgroup method divides the cross section itself into several sections which are called the subgroups, rather than dividing the energy

variable. After the subgroup parameters are obtained by either fitting method (Kitada et al., 1997) or moment method (Chiba and Unesaki, 2006), a neutron transport solver is employed to solve the subgroup slowing down equation in each single energy group to get subgroup flux. Then the multi-group averaged resonance cross sections can be obtained by utilizing the subgroup cross section and the subgroup flux.

In the subgroup method, subgroup parameters including subgroup cross section and subgroup probability are defined as follows

$$\sigma_{x,i,g} = \frac{\int_{\Delta E_i} \sigma_{x,g}(\mathbf{E}) \phi(\mathbf{E}) d\mathbf{E}}{\int_{\Delta E_i} \phi(\mathbf{E}) d\mathbf{E}} \quad (1)$$

$$p_{i,g} = \frac{\Delta E_i}{\Delta E_g} \quad (2)$$

where g and i index the multi-group and subgroup numbers respectively, $\sigma_{x,i,g}$ means the microscopic x subgroup cross section of group g and subgroup i . $\phi(\mathbf{E})$ means the flux spectra. $\sigma_{t,g}(\mathbf{E})$ means multi-group cross section of group g and the range of ΔE_i is $\Delta E_i \in \{\mathbf{E}/\sigma_{t,i} \leq \sigma_{t,g}(\mathbf{E}) \leq \sigma_{t,i+1}\}$.

The slowing down equation is transformed into the following form which is the same as the multi-group neutron transport equation (Liu, 2010)

$$\frac{d\phi_{g,i}(\mathbf{r}, \Omega)}{ds} + \Sigma_{t,g,i}(\mathbf{r}) \phi_{g,i}(\mathbf{r}, \Omega) = \mathbf{Q}_{g,i}(\mathbf{r}, \Omega) \quad (3)$$

$$\mathbf{Q}_{g,i}(\mathbf{r}, \Omega) = \mathbf{Q}_{s,g,i}(\mathbf{r}, \Omega) + \mathbf{Q}_{f,g,i}(\mathbf{r}, \Omega) \quad (4)$$

where $\phi_{g,i}(\mathbf{r}, \Omega)$ is flux in energy group g and subgroup i . $\Sigma_{t,g,i}(\mathbf{r})$ is macroscopic total subgroup cross section in energy group g and subgroup i . $\mathbf{Q}_{s,g,i}(\mathbf{r}, \Omega)$ and $\mathbf{Q}_{f,g,i}(\mathbf{r}, \Omega)$ are the scattering and fission sources from all the other energy groups to energy group g and subgroup i .

On one hand, all the geometric constrain lies in Eq. (2), which means that subgroup method can handle any geometry that the transport solver can handle. This is why SUGAR code employs the MOC solver which has the ability to treat arbitrary geometries.

On the other hand, the source term of Eq. (3) is contributed by all the other energy groups through scattering and fission. Hence, there is iteration with both fast and thermal energy groups getting involved even the resonance energy groups are the only targets. The iteration scheme is shown by Fig. 2.

Also, it can be seen that if there are more than two resonant nuclides, iteration is usually carried out to consider the interference effects between different nuclides and regions. Within each

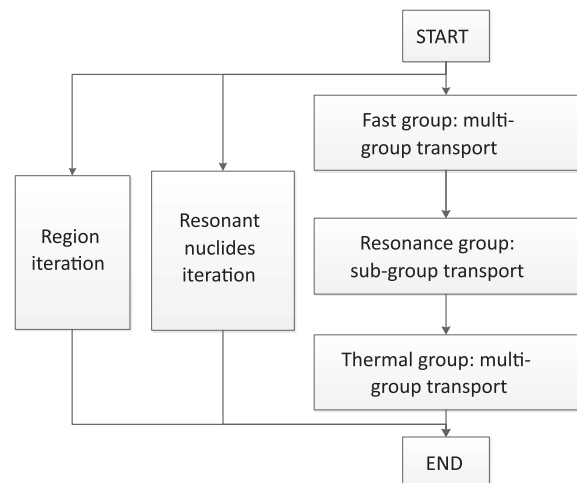


Fig. 2. The flowchart of iteration among fast group and thermal group.

iteration of this process, there is a loop between all the resonant nuclides. Within each loop, only one resonant nuclide is taken account with all the others treated as non-resonant nuclides. This iteration is terminated until all the interference effects are well handled. In some special cases, if there are different resonant nuclides in different regions, the region iteration is needed, which means taking resonant nuclides of one region as resonant nuclides while nuclides of other regions as non-resonant nuclides. However, if the materials of these two regions are the same, it is not necessary to iterate between these regions.

2.2. Problem independence of the subgroup parameters

Originally, the subgroup parameters have to be calculated specifically for each specific problem or even a specific case. However, it was found (Liu, 2010) that with the NR approximation employed, the group constant can be written into the following form:

$$\sigma_{x,g}(\sigma_0) \approx \frac{\sigma_{x,1g} \frac{P_{1g}}{(\sigma_{t,1g} + \sigma_0)} \cdots + \sigma_{x,Ng} \frac{P_{Ng}}{(\sigma_{t,Ng} + \sigma_0)}}{\frac{P_{1g}}{(\sigma_{t,1g} + \sigma_0)} \cdots + \frac{P_{Ng}}{(\sigma_{t,Ng} + \sigma_0)}} \quad (5)$$

where $\sigma_{x,g}(\sigma_0)$ is the microscopic cross section of group g , σ_0 is the dilution cross section. In SUGAR code, the max subgroup number is 3, so the max number of N is 3.

Along with Eq. (5), the subgroup parameters can be obtained if the multi-group cross sections with different dilution cross sections are given. Because the multi-group cross sections for different dilution cross sections in the library are problem independent, and the subgroup parameters only depend on isotope type and temperature. Thus, there is no need to calculate subgroup parameters iteratively during resonance calculation. These problem independent parameters can be pre-calculated and stored into the multi-group library to increase the computational efficiency of resonance calculation. For better efficiency, the number of subgroup is chosen automatically. In Eq. (5), the numerator and denominator in the formula can be written as multinomial which is shown as following

$$\sigma_{t,g}(\sigma_b) = \frac{c_2 \sigma_b^2 + c_1 \sigma_b \cdots + c_0}{d_2 \sigma_b^2 + d_1 \sigma_b \cdots + d_0} = \frac{c_2(\sigma_b + \mathbf{x}_1)(\sigma_b + \mathbf{x}_2)}{d_2(\sigma_b + \mathbf{x}_3)(\sigma_b + \mathbf{x}_4)} \quad (6)$$

where \mathbf{x}_i ($i = 1, 2$) is the solution if let numerator equal zero and \mathbf{x}_i ($i = 3, 4$) is the solution if let denominator equal zero. If $|\mathbf{x}_1 - \mathbf{x}_3| \leq \varepsilon$ or $|\mathbf{x}_2 - \mathbf{x}_4| \leq \varepsilon$, the subgroup number is two and the formula can be predigested as following

$$\sigma_{t,g}(\sigma_b) = \begin{cases} \frac{c_2(\sigma_b + \mathbf{x}_1)}{d_2(\sigma_b + \mathbf{x}_3)}, & |\mathbf{x}_2 - \mathbf{x}_4| \leq \varepsilon \\ \frac{c_2(\sigma_b + \mathbf{x}_2)}{d_2(\sigma_b + \mathbf{x}_4)}, & |\mathbf{x}_1 - \mathbf{x}_3| \leq \varepsilon \end{cases} \quad (7)$$

If $|\mathbf{x}_1 - \mathbf{x}_3| \leq \varepsilon$ and $|\mathbf{x}_2 - \mathbf{x}_4| \leq \varepsilon$ are both established, the subgroup number is one and the subgroup cross section equal multi-group cross section of same group.

2.3. If $|\mathbf{x}_1 - \mathbf{x}_3| \leq \varepsilon$ and $|\mathbf{x}_2 - \mathbf{x}_4| \leq \varepsilon$ are both not established, the subgroup number is three. Production of a multi-group library

Due to the demand of storing subgroup parameters and the increase of resonant nuclides, a new multi-group data library needs to be produced especially for the subgroup resonance calculation method.

For the new multi-group data library, firstly, a finer energy group structure is selected. The 361 groups format according to SHEM361 structure (Hébert and Santamarina, 2008) is introduced. Secondly, the number of resonant nuclides is extended. These fresh resonant nuclides are the long lived fission product isotopes like I-129, Se-79, Pd-107, Sn-126, Cs-125, and the burnable poison iso-

topes including Gd and Er, and some structure materials including Fe and Cu.

With the NJOY code, the multi-group library can be produced based on ENDF-BVII. For better accuracy, the scattering resonance is considered and resonance scattering integral table is produced. Meanwhile, a servo code is developed to transform formats, to maintain nuclide data files, to compute pseudo fission product isotopes, and so on. Its flow chart is shown in Fig. 3.

According to Section 2.2, the subgroup parameters are problem independent and can be treated beforehand. The generations of these subgroup parameters and multi-group cross sections can be completed together as Fig. 4.

2.4. Iteration optimization in subgroup method

As shown in Fig. 2, neutron slowing down equation for all the energy groups are coupled together due to the connections of scattering and fission source contributions. The resulting iteration between all the energy groups is pretty time consuming. But it was found that this iteration can be simplified by examining each of these connections.

Firstly, it is the fission source contribution. Summing the fission spectrum within fast energy range, it can be found that almost all the fission neutrons are fast ones

$$\sum_{g=1}^{55} \chi_g = 0.9995 \quad (8)$$

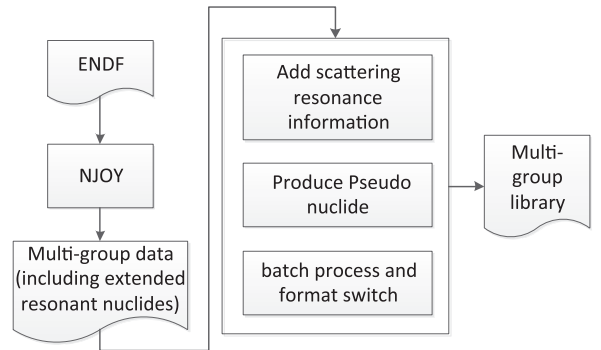


Fig. 3. The flow chart of producing multi-group library for subgroup method.

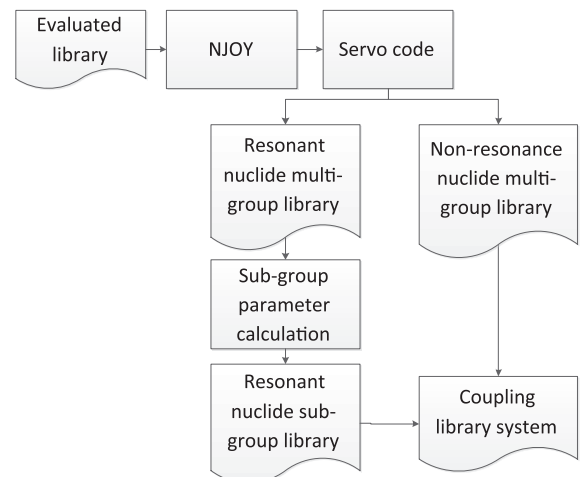


Fig. 4. The generations of subgroup parameters and multi-group cross sections for library.

Together with the assumption that neutron absorption and generation are separated by dividing the fission matrix into the vector product of neutron fission spectrum vector χ and macroscopic neutron production cross section vector $\nu\Sigma_f$, the fission connection between thermal and fast energy groups is decoupled.

Secondly, it is the up scattering source contribution. Examining the scattering matrix of each isotope within the new multi-group, it can be reasonably assumed that there is no up scattering within the resonance energy range.

The original source in the subgroup transport calculation is shown as Eq. (9).

$$\mathbf{Q} = \frac{1}{4\pi} \sum_{j=1,N} \int_{4\pi} \Sigma_{s,gj \rightarrow g,i} \times \phi_{gj}(\mathbf{r}, \Omega') d\Omega' + \mathbf{p}_i \left[\frac{1}{4\pi} \int_{4\pi} \Sigma_{s,g' \rightarrow g} \times \phi_{g'}(\mathbf{r}, \Omega') d\Omega' + \frac{1}{4\pi k} \sum_{g=1,G} \nu \Sigma_f(\mathbf{r}) \phi_g(\mathbf{r}) \right] \quad (9)$$

Through the two simplifications which have been shown above, the original source in the subgroup transport calculation could be simplified as following

$$\mathbf{Q} = \frac{1}{4\pi} \sum_{j=1,N} \int_{4\pi} \Sigma_{s,gj \rightarrow g,i} \times \phi_{gj}(\mathbf{r}, \Omega') d\Omega' + \mathbf{p}_i \left[(\mathbf{Q}_{s,g' \rightarrow g}(\mathbf{r}, \Omega)) \right]^0 \quad (10)$$

where $(\mathbf{Q}_{s,g' \rightarrow g}(\mathbf{r}, \Omega)) \right]^0$ is the initial value from high energy group and it does not need to update in each subgroup transport calculation.

The above two assumptions eliminates the fission and scattering contributions from low energy groups to high energy groups. Thus, the iteration as shown in Fig. 2 can be simplified into the one shown in Fig. 5 by sweeping the fast, resonance and thermal energy group only once.

This iteration optimization moves the fast group calculation and thermal group calculation out of the resonant nuclides iterations. When the iteration has been finished and the self-shielding cross section has been obtained, the multi-group transport calculation

follows to get the k-inf and multi-group flux. Thus, the speedup can be estimated as following:

$$\mathbf{a}_1^T = \frac{n(\mathbf{T}_{fast} + \mathbf{T}_{res} + \mathbf{T}_{thermal})}{\mathbf{T}_{fast} + n\mathbf{T}_{res} + \mathbf{T}_{fast} + \mathbf{T}_{res} + \mathbf{T}_{thermal}} \quad (11)$$

where \mathbf{a}_1^T is the speedup of iteration optimization and n is the iteration numbers, \mathbf{T}_{fast} , \mathbf{T}_{res} and $\mathbf{T}_{thermal}$ represent the computational time cost by transport calculations in the fast, resonance and thermal groups, which are proportional to their numbers of energy groups.

The iteration number depends on the number of resonant nuclides. So from the equation it can be seen that the more the iterations are, the larger the speedup is. In another word, the more the resonant nuclides are, the better the speedup of iteration optimization is.

2.5. Resonant nuclide grouping technique for resonance interference problem

The increase of resonant nuclides causes the low efficiency of legacy treatment. So it is necessary to consider how to keep efficiency and accuracy when resonant nuclides increase in calculation zone. The basic idea is that the large number of resonant nuclides could be classified into a small number of classes (Wemple et al., 2007) by grouping resonant nuclides with similar resonance characterizations rather than treating them as a single resonant nuclide.

According to the character of different resonant nuclides, they could be divided into several classes. Because of the similar peak width within one class, a pseudo nuclide is generated to represent all the resonant nuclides in this class. To generate this pseudo isotope, the resonance integral is preserved as shown in Eq. (12) after a typical isotope is chosen among the corresponding class

$$\Sigma_x(\sigma_{rep}) = \sum_i N_i \sigma_i = \sum_i N_i \frac{R_{i,\infty}}{R_{rep,\infty}} \sigma_{rep} = \left(\frac{\sum_i N_i R_{i,\infty}}{R_{rep,\infty}} \right) \sigma_{rep} \quad (12)$$

where $R_{rep,\infty}$ and $R_{i,\infty}$ are the resonance integrals of the typical and other resonant nuclides under the infinitude background cross section, σ_{rep} and σ_i are the corresponding subgroup cross section, N_i is the atomic density.

Normally, basing on nuclides characterizations, the resonant nuclides which have overlapping or part overlapping will be divided into same group.

For example, if there is a complicated fuel cell which contains U-235, U-238, Pu-239, Cs-133, Gd-154, Gd-155, Gd-156, Gd-157 and Gd-158, with the above resonant nuclides classified method and the class as shown in Table 1, only two pseudo resonant nuclides need to be iterated instead of the original nine isotopes.

What's more, considering from the regions and concentrations' point of view, some special nuclides which only occur in individual regions will be divided into same class. For example, Ag and In only occur in control rod and have high concentration, so they should be divided into a single class.

In SUGAR, subgroup cross sections and subgroup probability are all different in every resonance energy group. So compared with

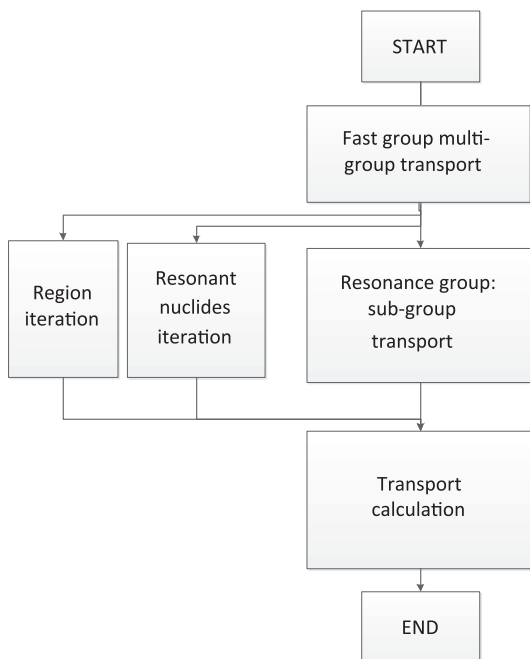


Fig. 5. The advanced flow chart of iteration calculation.

Table 1
Sort of nine resonant nuclides.

Resonant nuclides		Class
U-235	Gd-155	U-238(sort I)
U-238	Gd-156	U-235(sortII): (U-235,Pu-239,Cs-133,Gd-154,Gd-155,Gd-156,Gd-157,Gd-158)
Pu-239	Gd-157	
Cs-133	Gd-158	
Gd-154		

other subgroup resonance method (Wemple et al., 2007), because of different subgroup probability in every resonant nuclides, it is difficult to merger same group resonant nuclides' self-shield cross sections based on the typical resonance nuclides' subgroup flux when using the nuclides grouping technique. So, a new simple method is brought forward. The ideological kernel of the method is straight calculating the multi-group cross section instead of merging subgroup cross section. The calculation equation is shown as following,

$$\sigma_{i,self_shielding} = \frac{R_{i,\infty}}{R_{rep,\infty}} \sigma_{rep,self_reielding} \quad (13)$$

Here $\sigma_{rep,self_reielding}$ is typical nuclides' self shielding microscopic cross sections, $\sigma_{i,self_shielding}$ is other resonant nuclides' self shielding microscopic cross sections.

The speedup of this resonant nuclides group technique can be estimated as following

$$a_2^T = \frac{T_{fast} + mT_{res} + T_{fast} + T_{res} + T_{thermal}}{T_{fast} + nT_{res} + T_{fast} + T_{res} + T_{thermal}} \quad (14)$$

Here a_2^T is the speedup of resonant nuclides group technique, n and m are the iteration numbers before and after the utilization of this technique.

The original iteration number depends on the number of resonant nuclides. So from the equation it can be seen, the more the original iteration number, the better the speedup is. In another word, the more the resonant nuclides are, the better the speedup of resonant nuclides group technique is.

2.6. Neutron transport solver

As explained in Section 2.1, an in-house neutron transport solver named as AutoMOC was employed to solve the neutron slowing down equation as in Eq. (2) in the code SUGAR. At present, a matrix MOC solver named MMOC (Zhang et al., 2011) has been involved, which provides both the ability in handling arbitrary 2D geometry and superior computational efficiency.

According to the acceleration technique for 2D MOC based on Krylov subspace and domain decomposition methods, a speedup

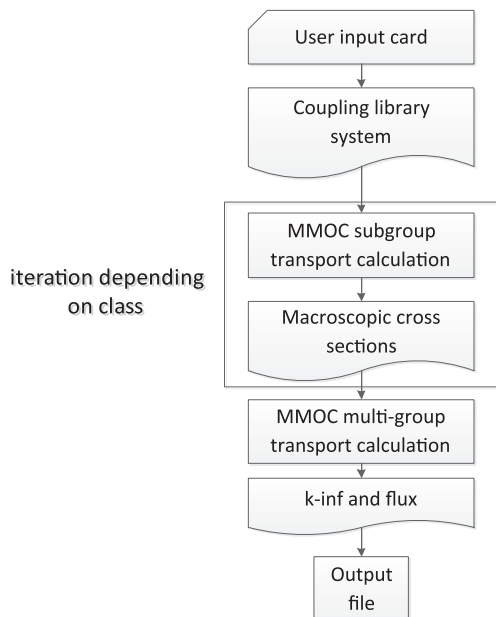


Fig. 6. Flow chart of subgroup resonance calculation.

of 1–10 can be achieved by replacing AutoMOC with MMOC (Zhang et al., 2011).

Finally, the new resonance calculation flow chart is obtained and is shown in Fig. 6.

3. Numerical results

In order to verify the above theories and the corresponding code development, a variety of resonance calculation benchmarks were employed, in which the large water hole, heterogeneous geometries, various of fuel types and enrichments are considered. All the calculations in this paper are carried out on a PC with Intel Core i7-2600 CPU (4 kernels, 3.40 GHz) and 2 G main memory.

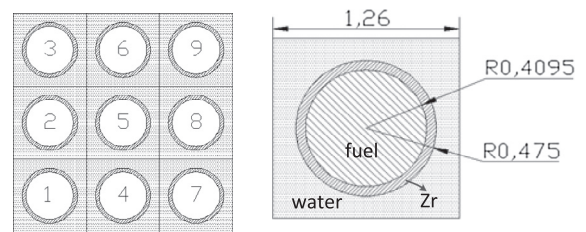


Fig. 7. 3 × 3 PWR assembly problem/cm.

Table 2
Cases of 3 × 3 assembly problem.

Pin cell	Case		
	1	2	3
1	UO ₂ -3%	UO ₂ -3%	UO ₂ -5%
2	UO ₂ -5%	UO ₂ -5%	UO ₂ -5%
3	UO ₂ -5%	UO ₂ -5%	UO ₂ -5%
4	UO ₂ -3%	UO ₂ -3%	UO ₂ -5%
5	UO ₂ -5%	Water	Water
6	UO ₂ -3%	UO ₂ -3%	UO ₂ -5%
7	UO ₂ -5%	UO ₂ -5%	UO ₂ -5%
8	UO ₂ -3%	UO ₂ -3%	UO ₂ -5%
9	UO ₂ -5%	UO ₂ -5%	UO ₂ -5%
	4	5	6
1	MOX-7%	MOX-7%	MOX-7%
2	MOX-7%	UO ₂ -5%	UO ₂ -5%
3	MOX-7%	MOX-7%	MOX-7%
4	MOX-7%	UO ₂ -5%	UO ₂ -5%
5	Water	UO ₂ -5%	Water
6	MOX-7%	UO ₂ -5%	UO ₂ -5%
7	MOX-7%	MOX-7%	MOX-7%
8	MOX-7%	UO ₂ -5%	UO ₂ -5%
9	MOX-7%	MOX-7%	MOX-7%

Table 3
Material atomic densities in six cases.

Nuclides	UO ₂ -5% ^a	MOX-7%	Water	Zr-nature
U-235	1.1547E-3	1.0913E-3	-	-
U-238	2.1939E-2	2.0474E-2	-	-
Pu-238	-	4.5730E-5	-	-
Pu-239	-	1.0124E-3	-	-
Pu-240	-	4.8224E-4	-	-
Pu-241	-	1.7458E-4	-	-
Pu-242	-	1.3126E-4	-	-
O-16	4.6187E-2	4.6823E-2	6.7233E-2	-
H-1	-	-	3.3617E-2	-
Zr-nature	-	-	-	4.3599E-2

^a 10²⁴ atoms/cm³.

Table 4
K-inf of the 3 × 3 PWR assembly problem.

Case	Monte Carlo	Original model	Advanced model	Original model error (%)	Advanced model error (%)
1	1.43959(0.00016)	1.43766	1.43847	0.134	0.078
2	1.45811(0.00016)	1.45645	1.45743	0.117	0.046
3	1.50550(0.00016)	1.50312	1.50402	0.159	0.098
4	1.35099(0.00015)	1.35291	1.35188	-0.142	-0.214
5	1.38610(0.00014)	1.38793	1.38704	-0.132	-0.284
6	1.40942(0.00014)	1.40956	1.41063	-0.009	-0.157

Table 5
The speedup of the six cases for the PWR problem.

Case	1	2	3	4	5	6
Original model(s)	261	293	270	607	614	679
Advanced model(s)	52	54	53	49	50	51
Speedup	5.0	5.4	5.1	12.4	12.2	13.3

3.1. 3×3. PWR assembly problem

This problem is from the literature benchmark problems and results for verifying resonance calculation methodologies (Wu et al., 2012). The geometry of 3 × 3 PWR assembly problem is shown in Fig. 7. The problem includes six cases shown in Table 2 and the material of each case is shown in Table 3. The six cases contain five sorts of cells and have different alternate collocation. The alternate collocation results in strong heterogeneity and has negative effect to resonance calculation accuracy.

The Monte Carlo method was used to provide the reference solution. In the Monte Carlo calculation, 20,000 particles are put for each generation and 300 generations are tallied, 50 of which are disregarded. The results of k-inf are shown in Table 4.

In order to check the results of iteration optimization, resonant nuclides grouping technique, and transport solver advance, the results of codes with and without these three improvements are compared. The speedup results are shown in Table 5.

From Table 4, it can be seen that compared with the Monte Carlo code, both the original and new codes can provide k-inf with relative error about 0.1% in the UO₂ fuel cases and less than 0.3% in the MOX fuel cases. For further verification, Fig. 8 compares the microscopic total cross sections of U-235 and U-238 in case 1 with the ones provided by Monte Carlo and SUGAR. The relative errors are almost less than 1% and 3–4% in several groups.

The 361 groups structure is employed in the transport solver, so the proportion of T_{fast} , T_{res} and $T_{thermal}$ can be obtained as $T_{fast}:-$

Table 6
The speedup of three kinds of improvements in six cases.

Case	1	2	3	4	5	6
a_1^T	1.6	1.6	1.6	1.6	1.6	1.6
a_2^T	-	-	-	2.1	2.1	2.1
a_3^T	3.1	3.4	3.2	3.7	3.6	4.0

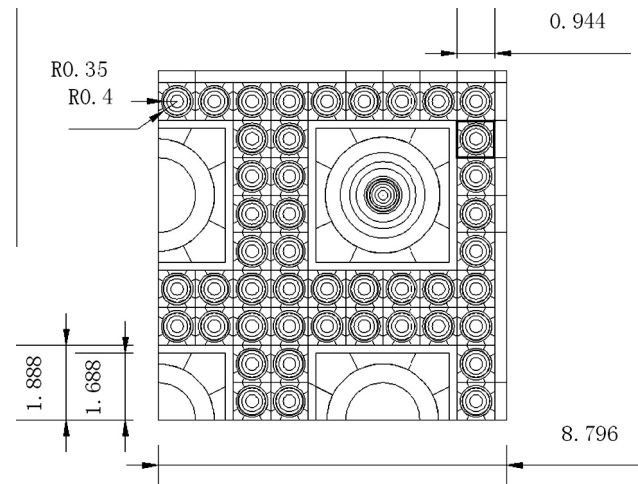
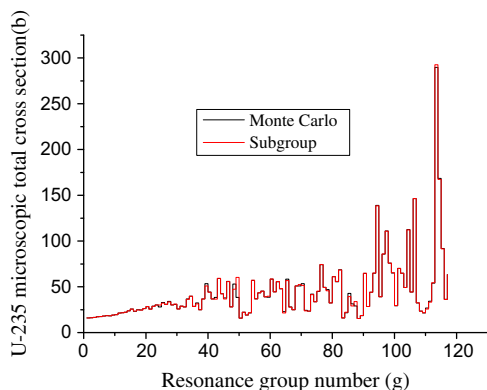


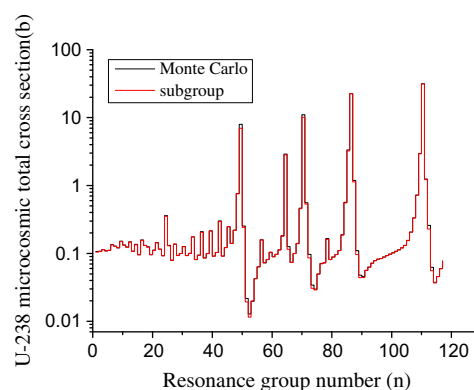
Fig. 9. Geometry of the SCWR assembly problem including the detail of resonance zone partition.

$T_{res}:T_{thermal} \approx 55:118:188$. By considering Eq. (11) in Section 2.4 and Eq. (14) in Section 2.5, the speedup estimation of iteration optimization is

$$a_1^T \approx \frac{361n}{118n + 416} \quad (15)$$



(a) U-235 microscopic total cross sections



(b) U-238 microscopic total cross sections

Fig. 8. Microscopic total cross sections of U-235 and U-238 in case 1.

And speedup estimation of resonant nuclides grouping technique is

$$a_2^T = \frac{118m + 416}{118n + 416} \quad (16)$$

And the speedup estimation of transport solver switch is

$$a_3^T = \frac{a_{total}^T}{a_1^T \times a_2^T} \quad (17)$$

here a_{total}^T is the total speedup obtained from Table 4.

For UO₂ cases from 1 to 3, there are 2 resonant nuclides and 4 iterations. For MOX cases from 4 to 6, there are 6 resonant nuclides and 12 iterations originally. In cases from 4 to 6, the resonant nuclides are divided into 2 groups and there are 4 iterations after the

utilization of the grouping technique. Therefore, the speedup of iteration optimization, resonant nuclides grouping technique and transport solver replacing can be obtained by using Eqs. (15)–(17), and listed in Table 6.

3.2. SCWR assembly problem

This problem comes from a super critical water assembly problem which contains large water holes (Zhao et al., 2013). Compared with other assembly problems, its heterogeneity is more prominent and its geometry is more complicated. Fig. 9 shows the geometry including the details of resonance zone partition used by SUGAR.

In order to test the resonant nuclides grouping technique, it is supposed that there are sufficient resonant nuclides in the fuel. In this case, the assembly contains 36 non-resonant nuclides and 16 resonant nuclides. The atomic densities of fuel can and water are shown in Table 7 and the fuel composition is shown in Table 8.

The results in Table 9 show that both the original and new codes agree well with the Monte Carlo method with relative error of about 0.2%. For further verification, one cell as marked in Fig. 9 is chosen to compare its microscopic total cross sections of U-235 and U-238. The comparisons are shown in Fig. 10. It can be found

Table 7
The atomic densities of can and water in SCWR.

Nuclides	Water in water hole ^a	Water in fuel pin cell	Can
O-16	2.5875E-02	3.3444E-03	–
H-1	5.1751E-02	6.6889E-03	–
Fe-nature	–	–	5.7287E-02

^a 10²⁴ atoms/cm³.

Table 8
The SCWR assembly fuel material detail.

Nuclides	Atomic density ^a	Nuclides	Atomic density	Nuclides	Atomic density	Nuclides	Atomic density
U-234	2.069E-08	Am-242	4.488E-10	Ag-109	7.759E-07	Sm-149	3.793E-08
U-235	1.404E-04	Am-243	2.629E-07	I-135	4.766E-09	Sm-150	2.492E-06
U-236	3.294E-05	Cm-242	5.535E-08	Xe-135	3.037E-09	Sm-151	1.686E-07
U-238	4.247E-03	Cm-243	1.047E-09	Cs-133	1.155E-05	Sm-152	8.712E-07
Np-237	2.784E-06	Cm-244	6.775E-08	Cs-134	1.044E-06	Eu-153	8.913E-07
Np-239	3.709E-07	Tc-99	1.087E-05	Cs-137	1.200E-05	Eu-154	1.868E-07
Pu-238	7.949E-07	Ru-101	9.983E-06	Nd-143	8.792E-06	Eu-155	5.394E-08
Pu-239	3.513E-05	Ru-103	5.018E-07	Nd-145	6.570E-06	Gd-154	3.413E-07
Pu-240	9.655E-06	Rh-103	5.416E-06	Pm-147	1.877E-06	Gd-155	4.047E-09
Pu-241	7.239E-06	Rh-105	1.145E-08	Pm-148	9.096E-09	Gd-156	6.635E-06
Pu-242	1.495E-06	Pd-105	3.945E-06	Pm-149	9.721E-09	Gd-157	6.816E-09
Am-241	2.347E-07	Pd-108	1.254E-06	Sm-147	7.332E-07	Gd-158	7.473E-06

^a 10²⁴ atoms/cm³.

Table 9
K-inf of the SCWR assembly problem.

Monte Carlo (standard deviation)	Original model	Advanced model	Original model error (%)	Advanced model error (%)
0.68019(0.00016)	0.67895	0.67912	0.18	0.18

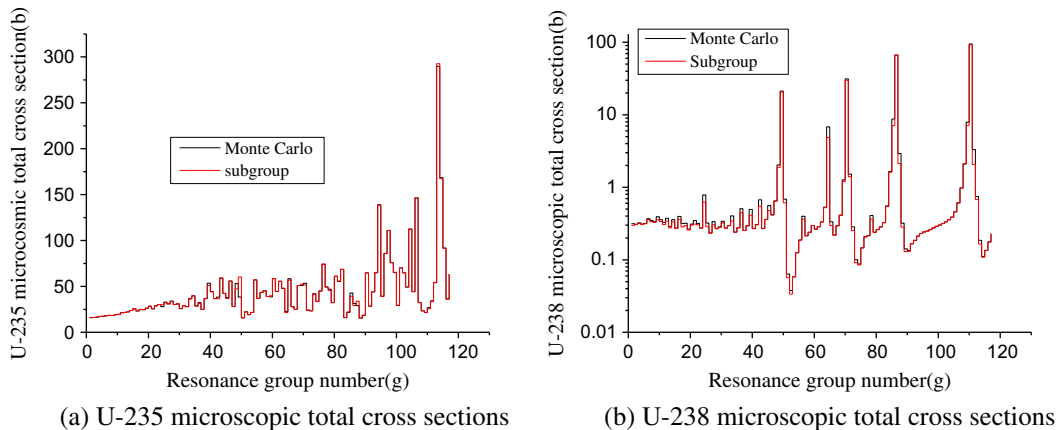


Fig. 10. U-235 and U-238 microscopic cross section of complicated fuel in SCWR.

Table 10

The speedup of SCWR assembly calculation.

Case	Original model(s)	Advanced model(s)	Speedup
SCWR assembly	21,792	665	32.8

Table 11

The speedup of three improvements for the SCWR assembly problem.

Improved model	α_1^T	α_2^T	α_3^T
SCWR assembly	1.6	4.7	4.4

that the results agree well with the results of Monte Carlo calculation. The speedup result is shown in Table 10.

There are 16 resonant nuclides and 32 iterations for the original code. The resonant nuclides are divided into 2 groups and the iteration number is 4 for the new code. Finally the speedup of iteration optimization, resonant nuclides grouping technique and transport solver replacing are shown in Table 11.

Compared with the original one, the improved version of SUGAR runs faster by a factor of about 32.8 in this problem, which is higher than the one for the 3×3 PWR assembly problem. There are two reasons that can be found from the separated speedup. First, it is clear that the speedup of resonant nuclides grouping technique in SCWR problem is larger than that of the 3×3 PWR assembly problems (4.7 and 2.1 respectively). Second, the speedup of transport solver replacement is higher than that in 3×3 PWR assembly problems (4.4 and 4.0 respectively), since the MMOC code is more suitable for solving the complicated geometry problems.

4. Conclusion

In order to improve the efficiency of subgroup resonance calculation code SUGAR, this paper first produces a multi-group library in SHEM-361 format, then produce the problem-independent subgroup parameters, proposes an algorithm of automatically choosing of subgroup number. Based on the two assumptions, the iteration process within subgroup method is simplified. Aiming at multi-nuclide resonance problem, this paper employs the resonant nuclides grouping technique. In addition, the neutron slowing down equation solver is upgraded to a matrix MOC solver from the original one, which obviously improves the computational efficiency with geometric flexibility maintained.

From the theoretical analysis and the verification results, the holistic speedups of these four improvements to the SUGAR code is about 5–32. The speedup of iteration optimization depends on the number of multi-nuclide resonance iteration. It is about 1.6 for both the 3×3 PWR assembly problem and SCWR assembly problem. The speedup of resonant nuclides grouping technique depends on the number of resonant nuclides and number of resonant nuclides groups. It is about 2.1 in the MOX fuel calculation with 6 resonant nuclides and about 4.7 in the SCWR assembly calculation with 16 resonant nuclides. In this paper, the speedup of MMOC is 3.1–4.4 compared with the original solver. The results show that the advanced model can effectively increase the calculation efficiency of subgroup code SUGAR and meanwhile keeps enough accuracy and geometric flexibility. It is also found that the more the resonant nuclides are, the better the speedup is.

These improvement scan also be extended to other resonance methods. The iteration optimization can be used in which the

two assumptions in Section 2.4 can be used in group iterations when the transport equation or slowing down equation is employed as a solver for flux, including some multi-group resonance method and wavelet expansion method. The resonant nuclides grouping technique can be used in multi-group resonance calculation methods when there are many resonant nuclides in the multi-nuclide resonance iteration.

Acknowledgements

This work is supported by the National Natural Science Foundation of China (Approved numbers 91126005 and 91226106).

References

- Cao, Liangzhi., Wu, Hongchun., Liu, Qingjie., 2011. Arbitrary Geometry Resonance Calculation Using Subgroup Method and Method of Characteristics. M&C 2011, Brazil.
- Chen, Qichang., Wu, Hongchun., Cao, Liangzhi., 2008. auto moc-a 2d neutron transport code for arbitrary geometry based on the method of characteristics and customization of AutoCAD. Nucl. Eng. Des. 238 (10), 2828–2833.
- Chiba, G., Unesaki, H., 2006. Improvement of moment-based probability table for resonance self-shielding calculation. Ann. Nucl. Energy 33 (13), 1141–1146.
- Dahmani, M., Marleau, G., Le Tellier, R., 2008. Modeling reactivity devices for advanced CANDU reactors using the code DRAGON. Ann. Nucl. Energy 35 (5), 804–812.
- Franceschini, F., Petrovic, B., 2008. Core physics analysis of 100% MOX core in IRIS. Ann. Nucl. Energy 35 (9), 1587–1597.
- He, Lei., Wu, Hongchun., Cao, Liangzhi., et al., 2010. Multi-Group Library Generation for the Study of Nuclide Transmutation in High Flux Engineering Test Reactor. ICONE18-29563, Xi'an, China.
- Hébert, A., 2009. Development of the subgroup projection method for resonance self-shielding calculation. Nucl. Sci. Eng. 162 (1), 56–75.
- Hébert, A., Santamarina, A., 2008. Refinement of the Santamarina-Hfaiedh Energy Mesh between 22.5 eV and 11.4 keV. PHYSOR 2008, Switzerland.
- Ishiguro, Y., 1973. Neutron resonance-absorption in heterogeneous fast-reactor assemblies. Nucl. Sci. Eng. 51 (4), 441–455.
- Jeong, C.J., Suk, H.C., 2002. Assessment of core characteristics during transition from 37-element fuel to CANFLEX-NU fuel in CANDU6. Ann. Nucl. Energy 29 (1), 1721–1733.
- Kitada, T., Kuroda, M., Takeda, T., 1997. Improvement of fitting method of multiband parameters for cell calculations. J. Nucl. Sci. Technol. 34 (7), 638–643.
- Le Tellier, R., Fournier, D., Ruggieri, J.M., 2009. A wavelet-based finite element method for the self-shielding issue in neutron transport. Nucl. Sci. Eng. 163 (1), 34–55.
- Liu, Qingjie., 2010. Sub-Group Resonance Calculation Method and Its Application in the Two Dimensional Arbitrary Geometry. Xi'an Jiaotong University, Xi'an.
- Misu, S., Grummer, R.G., 1997. Calculation of BWR cycles with CASMO-3-MICROBURN-B and comparison with measurements. Nucl. Eng. Des. 170 (1–3), 183–191.
- Patrulescu, I., Constantin, M., Rades, E., et al., 1997. Development of CANDU reactor physics calculation system based on WIMS code. Ann. Nucl. Energy 24 (14), 1105–1125.
- Salvatore, M., 2005. Nuclear fuel cycle strategies including partitioning and transmutation. Nucl. Eng. Des. 235 (7), 805–816.
- Takeda, T., Yokoyama, K., 1997. Study on neutron spectrum for effective transmutation of minor actinides in thermal reactors. Ann. Nucl. Energy 24 (9), 705–719.
- Trkov, A., Ravnik, M., 1993. Application of ENDF/B-VI data for the WIMS lattice code. Ann. Nucl. Energy 20 (8), 561–568.
- Tsuchihashi, K., 1989. Development validation and applications of SRAC-JAERI thermal reactor standard neutronics code system. J. Nucl. Sci. Technol. 26 (1), 23–27.
- Wemple, C.A., Stamm'ler, R.J.J., Ferri, A.A., 2007. Improved temperature-dependent resonance treatment in HELIOS-1.9. Trans. Am. Nucl. Soc. 96, 657–659.
- Wu, Hongchun., Yang, Weiyang., Qin, Yulong., He, Lei., 2012. Benchmark Problems and Results for Verifying Resonance Calculation Methodologies. Physor2012, Tennessee, USA.
- Yang, Weiyang., Wu, Hongchun., Zheng, Youqi., Cao, Liangzhi., 2010. Application of wavelets scaling function expansion method in resonance self-shielding calculation. Ann. Nucl. Energy 37 (5), 653–663.
- Zhang, Hongbo, Wu, Hongchun, Cao, Liangzhi., 2011. An acceleration technique for 2D MOC based on Krylov subspace and domain decomposition methods. Ann. Nucl. Energy 38 (12), 2742–2751.
- Zhao, Chuanqi, Cao, Liangzhi, Wu, Hongchun., 2013. Conceptual design of a supercritical water reactor with double-row-rod assembly. Prog. Nucl. Eng. 63, 86–95.